

Hierarchical Refinement of Latin Hypercube Samples

Miroslav Vořechovský*

Faculty of Civil Engineering, Institute of Structural Mechanics, Brno University of Technology, Veveří 95, 602 00, Brno, Czech Republic

Abstract: *In this article, a novel method for the extension of sample size in Latin Hypercube Sampling (LHS) is suggested. The method can be applied when an initial LH design is employed for the analysis of functions g of a random vector. The article explains how the statistical, sensitivity and reliability analyses of g can be divided into a hierarchical sequence of simulations with subsets of samples of a random vector in such a way that (i) the favorable properties of LHS are retained (the low number of simulations needed for statistically significant estimations of statistical parameters of function g with low estimation variability); (ii) the simulation process can be halted, for example, when the estimations reach a certain prescribed statistical significance. An important aspect of the method is that it efficiently simulates subsets of samples of random vectors while focusing on their correlation structure or any other objective function such as some measure of dependence, spatial distribution uniformity, discrepancy, etc. This is achieved by employing a robust algorithm based on combinatorial optimization of the mutual ordering of samples. The method is primarily intended to serve as a tool for computationally intensive evaluations of g where there is a need for pilot numerical studies, preliminary and subsequently refined estimations of statistical parameters, optimization of the progressive learning of neural networks, or during experimental design.*

1 INTRODUCTION

Statistical sampling is of interest not only to statisticians but also to practitioners in a variety of research fields such as engineering, economics, design of experiments, and operational research. The evaluation of the uncertainty associated with analysis outcomes is now widely recognized as an important part of any modeling effort. A number of approaches to such evaluation are in use, including differential analysis (Cacuci, 2003;

Tamás, 1990; Rabitz et al., 1983; Frank, 1978; Katafygiotis and Papadimitriou, 1996; Brząkała and Puła, 1996), neural networks (Zhou et al., 2013; Fuggini et al., 2013; Graf et al., 2012; Panakkat and Adeli, 2009; Adeli and Park, 1996), fuzzy set theory and fuzzy variables (Reuter and Möller, 2010; Sadeghi et al., 2010; Anoop et al., 2012; Hsiao et al., 2012), variance decomposition procedures (Li et al., 2001; Rabitz and Ali, 1999), and Monte Carlo (i.e., sampling-based) procedures (Sadeghi et al., 2010; Yuen and Mu, 2011; Hammersley and Handscomb, 1964; Rubenstein, 1981; Kalos and Whitlock, 1986; Sobol', 1994). Another common task is to build a surrogate model to approximate the original, complex model, for example, a response surface (Myers et al., 2004; Myers, 1999; Andres, 1997; Sacks et al., 1989; Mead and Pike, 1975; Myers, 1971), a support vector regression or a neural network (Novák and Lehký, 2006). The surrogate model is based on a set of carefully selected points in the domain of variables; see, for example Dai et al. (2012). Simulation of random variables from multivariate distributions is also needed in the generation of random fields (Vořechovský, 2008).

Conceptually, an analysis can be formally represented by a deterministic function, $Z = g(X)$, which can be a computational model or a physical experiment (which is expensive to compute/evaluate) and where Z is the uncertain response variable or a vector of outputs. In this article, Z is considered to be a random variable (vector). The vector $X \in \mathbb{R}^{N_{\text{var}}}$ is considered to be a random vector of N_{var} marginals (input random variables describing uncertainties/randomness).

Other than the multivariate normal distribution, few random vector models are tractable and general, though many multivariate distributions are well documented (Johnson, 1987). A review of the available techniques for the simulation of (generally non-Gaussian) correlated vectors are listed in a paper by Vořechovský and Novák (2009). The information on the random vector X is therefore usually limited to marginal probability density functions (PDFs), $f_i(x)$ ($i = 1, \dots, N_{\text{var}}$), and a

*To whom correspondence should be addressed. E-mail: vorechovsky.m@fce.vutbr.cz.

correlation matrix, T (a symmetric squared matrix of the order N_{var}):

$$T = \begin{matrix} & X_1 & X_2 & \dots & X_{N_{\text{var}}} \\ \begin{matrix} X_1 \\ X_2 \\ \vdots \\ X_{N_{\text{var}}} \end{matrix} & \begin{pmatrix} 1 & T_{1,2} & \dots & T_{1,N_{\text{var}}} \\ \vdots & 1 & \dots & \vdots \\ \vdots & \vdots & \ddots & \vdots \\ \text{sym.} & \dots & \dots & 1 \end{pmatrix} \end{matrix} \quad (1)$$

Suppose the analytical solution to the transformation $g(\mathbf{X})$ of the input variables is not known. The task is to perform statistical, sensitivity, and possibly reliability analysis of $g(\mathbf{X})$ given the information above. In other words, the problem involves the estimation of statistical parameters of response variables and/or theoretical failure probability.

Statistical and probabilistic analyses can be viewed as estimations of probabilistic integrals. Given the joint PDF of the input random vector $f_X(\mathbf{x})$, and the function $g(\mathbf{X})$, the estimate of the statistical parameters of $g(\cdot)$ is, in fact, an approximation to the following integral:

$$\int_{-\infty}^{\infty} \dots \int_{-\infty}^{\infty} S[g(\mathbf{X})] f_X(\mathbf{X}) dX_1 dX_2 \dots dX_{N_{\text{var}}} \quad (2)$$

where the particular form of the function $S[g(\cdot)]$ depends on the statistical parameter of interest. To gain the mean value, $S[g(\cdot)] = g(\cdot)$, higher statistical moments of the response can be obtained by integrating polynomials of $g(\cdot)$. The probability of failure is obtained in a similar manner; $S[\cdot]$ is replaced by the Heaviside function (or indicator function) $H[-g(\mathbf{X})]$, which equals one for a failure event ($g < 0$) and zero otherwise. In this way, the domain of integration of the joint PDF above is limited to the failure domain.

Many techniques have been developed in the past to approximate such integrals. The most prevalent technique is Monte Carlo simulation (MCS). MCS is popular for its simplicity and transparency and is also used as a benchmark for other (specialized) methods. In Monte Carlo-type techniques, the above integrals are numerically estimated using the following procedure: (1) draw N_{sim} realizations of \mathbf{X} that share the same probability of $1/N_{\text{sim}}$ by using its joint distribution $f_X(\mathbf{x})$ (the samples are schematically illustrated by the columns in Figure 1); (2) compute the same number of output realizations of $S[g(\cdot)]$; and (3) estimate the results as statistical averages. The disadvantage of crude MCS is that it requires a large number of simulations (i.e., the repetitive calculation of responses) to deliver statistically significant results. This becomes unfeasible when the analysis requires time-consuming evalua-

tion (in the form of a numerical or physical experiment). In this respect, minimization of the number of simulations is essential. This can be obtained in two ways: (1) sampling should be highly efficient so that the desired accuracy level is attained with a minimal number of simulations and, (2) sampling convergence should be easily quantified so that the analysis can be halted once suitably accurate results have been obtained.

Since $g(\cdot)$ is expensive to compute (or otherwise evaluate), it is advantageous to use a more complicated sampling scheme. The selection of sampling (integration) points should be optimized so as to maximize the amount of important information that can be extracted from the output data. Note that when sampling from random vectors, it is important to control correlations or some other dependence patterns between marginals (copulas, etc.) as many models are sensitive to correlations among inputs.

A good choice is one of the “variance reduction techniques,” a stratified sampling strategy called Latin Hypercube Sampling (LHS). LHS was first suggested by W. J. Conover, whose work was motivated by the time-consuming nature of simulations connected with the safety of nuclear power plants. Conover’s original unpublished report (Conover, 1975) is reproduced as appendix A of Helton and Davis (2002) together with a description of the evolution of LHS as an unpublished text by R. L. Iman (1980). LHS was formally published for the first time in conjunction with Conover’s colleagues (McKay et al., 1979; Iman and Conover, 1980).

It has been found that stratification with proportional allocation never increases variance compared to crude MCS, and can reduce it. McKay et al. (1979) showed that such a sample selection reduces the sampling variance of the statistical parameters of $g(\mathbf{X})$ when $g(\cdot)$ is monotone in each of the inputs. Iman and Conover (1980) showed that for an additive model in which all the inputs have uniform density functions, the variance of the estimated mean converges at $O(N_{\text{sim}}^{-3})$ for LHS, which is significantly better than $O(N_{\text{sim}}^{-1})$, which is obtained for crude MCS. Later, Stein (1987) showed that LHS reduces the variance compared to simple random sampling (crude MCS) and explained that the amount of variance reduction increases with the degree of additivity in the random quantities on which the function $g(\mathbf{X})$ depends.

The LHS strategy has been used by many authors in different fields of engineering and with both simple and very complicated computational models (Duthie et al., 2011; Marano et al., 2011; Hegenderfer and Atamturk, 2012; Chudoba et al., 2013). LHS is especially suitable for statistical and sensitivity calculations. However,

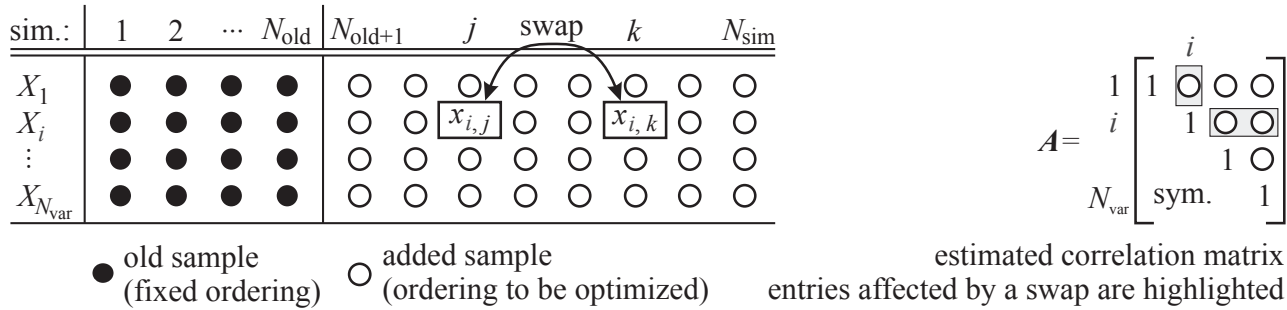


Fig. 1. Left: Extension of sample size with correlation control over the extended part. Right: Estimated correlation matrix with highlighted entries affected by a swap.

it is possible to use the method for probabilistic assessment if curve fitting is employed. LHS has also been successfully combined with the importance sampling technique (Olsson et al., 2003) to minimize the variance of estimates of failure probability by sampling importance density around the design point (the most probable point on limit state surface $g(X) = 0$). Optimal coverage of a sample space consisting of many variables with a minimum of samples is also an issue in the theory of design of experiments, and LHS and related sampling techniques have their place in that field.

When using LHS, the choice of sample size is a practical difficulty. A small sample size may not give acceptable statistically significant results, while a large sample size may not be feasible for simulations that take hours to compute. Examples of such complicated computations include models in computational fluid dynamics, crashworthiness models based on the finite element method, and models used in the statistical analysis of nonlinear fracture mechanics problems (Bažant et al., 2007; Vořechovský and Sadílek, 2008; among others), see also the numerical example in this article. In many such computer analyses it is impossible to determine the sample size needed to provide adequate data for statistical analysis *a priori*. Therefore, the ability to extend and refine the design of an experiment may be important. It is thus desirable to start with a small sample and then extend (refine) the design (using more samples during the estimation of integrals) if it is deemed necessary. One needs, however, a sampling technique in which pilot analyses can be followed by an additional sample set (or sets) without the need to discard the results of the previous sample set(s). The problem is depicted in Figure 1, where the extension of the sampling plan is illustrated by empty circles.

Note that in crude MCS the continuous addition of new sample subsets to an existing set can be performed without any violation of the consistency of the whole sample set. However, if some kind of variance reduc-

tion technique is used (such as LHS), one has to proceed with special care.

This article describes a simple technique for the sample extension of an LH-sample. The article is based on an earlier publication by the author Vořechovský (2006), which saw minor updates in Vořechovský (2009, 2012b). A related extension technique for LHS was developed at the same time by Tong (2006), but it does not consider correlated variables. Another related paper was produced by Sallaberry et al. (2008), who described a method for doubling the sample size (by replicating the samples) in LHS while employing a form of correlation control over the input random variables. Later, a related technique appeared in the literature Qian (2009) under the name *nested Latin hypercube design*. A nested LH-design with two layers is defined as being a special LH-design that contains a smaller LH-design as a subset. The need to extend the sample size in LHS (to “inherit an existing LH-sample”) also arose during the building of a sparse polynomial chaos expansion for stochastic finite element analysis (Blatman and Sudret, 2010). Their technique, however, may not yield a true LH-sample with uniformly represented probabilities.

The present article starts with a review of standard LHS in Section 2. The development of the refinement technique for a single random variable is presented in Section 3. Section 4 extends the approach to multivariate cases by employing an advanced correlation control algorithm. The rest of the article presents numerical convergence studies and a comparison of the performance of the refinement technique with that of standard LHS.

2 STANDARD LHS

LHS is a special type of MCS which uses the stratification of the theoretical probability distribution functions

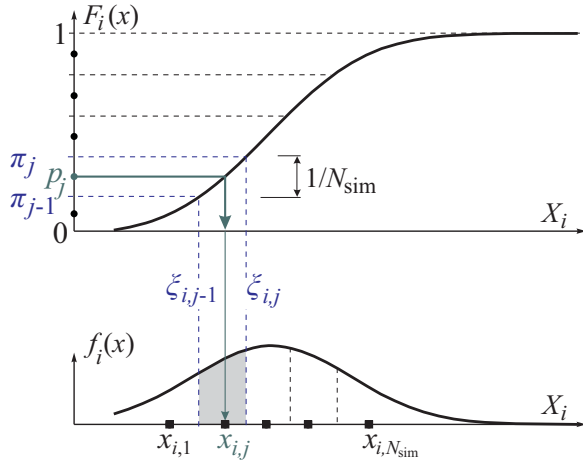


Fig. 2. Sample selection for a single random variable in LHS.

of individual marginal random variables in such a way that the region of each random variable X_i is divided into N_{sim} contiguous intervals of equal probability, indexed by $j = 1, \dots, N_{sim}$, in consistency with the corresponding distribution function F_i ; see Figure 2. This is achieved by dividing the unit probability interval into N_{sim} probability intervals of identical length (probability), $1/N_{sim}$. Each j th interval is bounded by the lower probability bound π_{j-1} and upper probability bound π_j , where

$$\pi_j = j/N_{sim}, \quad j = 1, \dots, N_{sim} \quad (3)$$

The corresponding interval over the values of variable X_i , from which one representative x_j must be selected, is bounded (see Figure 2) so that $x_j \in \langle \xi_{i,j-1}, \xi_{i,j} \rangle$, where

$$\xi_{i,j} = F_i^{-1}(\pi_j), \quad i = 1, \dots, N_{var}, \quad j = 1, \dots, N_{sim} \quad (4)$$

There are several alternative ways of selecting the sample values from these intervals (Vořechovský and Novák, 2009). One such option is to generate a random sampling probability for each interval bounded by $\langle \pi_{j-1}, \pi_j \rangle$ and perform an inverse transformation of the distribution function, such as the one in Equation (4). Another option is to select the mean value from each interval (the centroid of the shaded area in Figure 2) as in (Keramat and Kielbasa, 1997; Huntington and Lyrintzis, 1998):

$$x_{i,j} = \frac{\int_{\xi_{i,j-1}}^{\xi_{i,j}} x f_i(x) dx}{\int_{\xi_{i,j-1}}^{\xi_{i,j}} f_i(x) dx} = N_{sim} \int_{\xi_{i,j-1}}^{\xi_{i,j}} x f_i(x) dx \quad (5)$$

Sampling plan for two random variables:

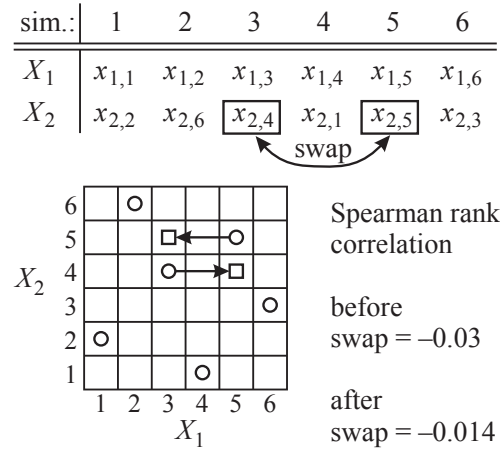


Fig. 3. Illustration of a random trial in the correlation control algorithm—a swap of samples j and k of variable X_2 .

In this article, the most commonly used strategy is preferred: the *median* of each interval is selected by taking the following set of sampling probabilities:

$$\mathbf{p} = \{p_1, p_2, \dots, p_j, \dots, p_{N_{sim}}\}: \quad p_j = \frac{j - 0.5}{N_{sim}} \quad (6)$$

These *sampling probabilities* form a regular grid over the unit probability region; see the solid circles in Figure 2. They can be used to form an $N_{var} \times N_{sim}$ matrix P of sampling probabilities $P_{i,j}$, where each row is a permutation of the vector of sampling probabilities \mathbf{p} . The samples of arbitrary continuously distributed variable $X_i \sim P(X_i \leq x) \equiv F_i(x)$ are selected using the inverse transformation of the probabilities (entries) in matrix P :

$$x_{i,j} = F_i^{-1}(P_{i,j}), \quad i = 1, \dots, N_{var}, \quad j = 1, \dots, N_{sim} \quad (7)$$

These samples then form a *sampling plan*: a matrix of the dimensions $N_{var} \times N_{sim}$ that contains the values selected from \mathbf{X} ; see the solid circles in Figure 1 for a diagram of the sampling plan for four random variables and four simulations. Another example of a sampling plan but with two random variables and six simulations can be found in Figure 3.

At the beginning of the process, sampling probabilities \mathbf{p} from Equation (6) are sorted in ascending order. They form rows in P . In LHS it is necessary to minimize the difference between the target correlation matrix, T , and the actual correlation matrix, A , which is estimated from the generated sample. The difference between these two matrices can be quantified by a suitable matrix norm (see, Vořechovský and Novák,

2009). This matrix norm can be minimized by changing the mutual ordering of the samples in the sampling plan; see the illustration of a swap in Figure 3. Many authors use random permutations to diminish undesired correlation between variables, though this method has been shown (Vořechovský, 2012a) to deliver relatively large errors in correlation with small sample sizes. Therefore, Vořechovský and Novák (2009) proposed a combinatorial optimization algorithm based on simulated annealing to control correlations among sampling plan rows. This rank optimization method seems to be the most efficient technique for exercising correlation control over samples of univariate marginals with fixed values. In the following study it is shown how the algorithm may also be exploited to optimize the ranking of the extended part of the sampling plan; see the empty circles in Figure 1.

Let us assume that the initial LH-sampling plan already exists and that the task is to add new simulations to it so that the aggregated sample will be a true LH-sample. It is proposed that this be achieved in two steps: (1) the extension of the sample for each univariate marginal variable X_i , $i = 1, \dots, N_{\text{var}}$, and (2) the optimization of the order of the added samples for each variable to control the dependence pattern of the whole sample (i.e., to control the spatial distribution of the points). These two steps are described in the following two subsections.

3 SAMPLE SIZE EXTENSION ALGORITHM: UNIVARIATE SAMPLING

In this section, a particular design for an aggregated sample set denoted as HLHS is described and proposed. The abbreviation stands for hierarchical Latin Hypercube Sampling. In this method, the previously selected sampling probabilities from Equation (6) constitute the *parent subset*, \mathbf{p}_{old} . Its *child subset*, \mathbf{p}_{add} , is constructed in such a manner that each sampling probability of \mathbf{p}_{old} will “generate” t offspring sampling probabilities. The additional subsets themselves are not LH-samples. However, if such a subset is combined with the previous subset, one obtains an *exact* LH-sample set, \mathbf{p}_{tot} . The size of the preceding LH-sample can be arbitrary.

The extension of the sample for each random variable can be performed for arbitrary distribution F_i because this distribution function transforms the desired density into a uniform distribution over the interval $(0, 1)$. Since the property of the one-dimensional uniformity of sampling probabilities is going to be preserved in HLHS, the problem is reduced to finding a regular grid over the unit probability interval $(0, 1)$. If the aggregated sample is truly an LH-sample with uniformly distributed

sampling probabilities, the extended sample size must be obtained either by (1) replicating the same sampling probabilities or by (2) adding new sampling probabilities in such a way that the aggregated vector of sampling probabilities will form a regular grid. The second option has been selected for HLHS because it is argued that designs should be “noncollapsing.” When one of the input variables has (almost) no influence on the black-box function $g(\cdot)$, two design points that differ only in this parameter will “collapse,” that is, they can be considered as being the same sampling point that is evaluated twice. This is not a desirable situation. Moreover, as shown by Hansen et al. (2012), a replicated sample (a sample obtained with identical sampling points that have been mutually reordered) may not bring any additional information. Therefore, two design points should not share any coordinate values when it is not known *a priori* which parameters are important. The proposed HLHS method fulfills this requirement.

Let us use the following notation:

$$\mathbf{p}_{\text{tot}} = \mathbf{p}_{\text{old}} \cup \mathbf{p}_{\text{add}} \quad (8)$$

where \mathbf{p}_{old} is the existing LH-sample with N_{old} simulations, \mathbf{p}_{add} is the extension of the LH-sample with N_{add} simulations, and \mathbf{p}_{tot} is the aggregated vector of sampling probabilities with N_{sim} simulations:

$$N_{\text{sim}} = N_{\text{old}} + N_{\text{add}} \quad (9)$$

Let t denote the *refinement factor*, where t is a positive even integer. The added sample size is

$$N_{\text{add}} = t N_{\text{old}} \quad (10)$$

so that

$$N_{\text{sim}} = N_{\text{old}} + N_{\text{add}} = (t + 1)N_{\text{old}} \quad (11)$$

The smallest possible value of t is two, which means that double the already sampled values are added to the current set; see Figure 4 left. The total sample size is then $N_{\text{sim}} = 3N_{\text{old}}$. Since the sample can be refined repeatedly (hierarchically), the slowest addition ($t = 2$) leads to the following sample size after r extensions:

$$N_{\text{sim}} = 3^r N_{\text{old}} \quad (12)$$

In order to achieve the uniform distribution of sampling probabilities in $\mathbf{p} \equiv \mathbf{p}_{\text{tot}}$ given in Equation (6), the sampling probabilities that were already used in set \mathbf{p}_{old} must be ignored. In particular, to obtain \mathbf{p}_{add} , all indices $j = 1, \dots, N_{\text{sim}}$ that follow the equality

$$(j - 1) \pmod{(t + 1)} = t/2, \quad (13)$$

must be ignored as they are already present in \mathbf{p}_{old} . Here, $a \pmod{b}$ is the modulo operation; $a \pmod{b}$ is the remainder of the Euclidean division of a by b . When, for example, $t = 2$, the following indices are

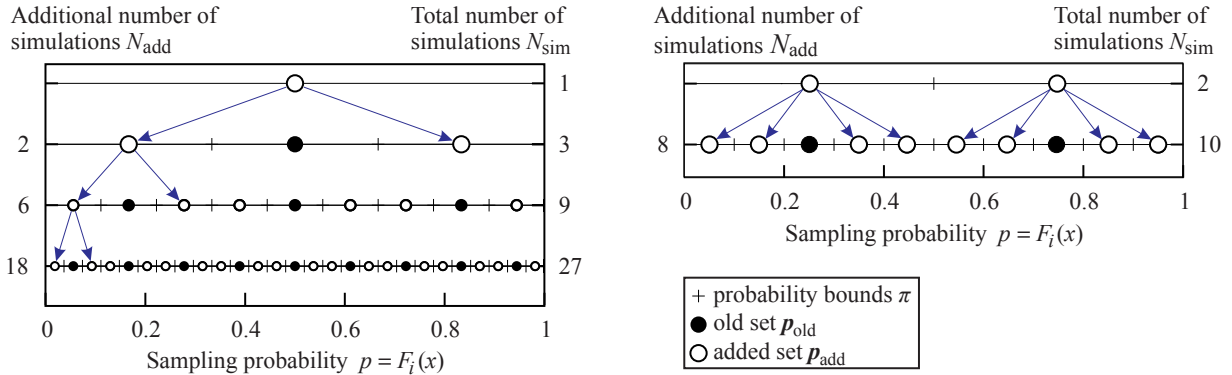


Fig. 4. Hierarchical Latin Hypercube Sample. Left: Hierarchy of three refinements ($t = 2$) of an initial design with one sample. Right: One step in the extension of sample size with the refinement factor $t = 4$ and an initial design with two samples.

```

int idx = Nold; //index in 'p' array is set equal the old sample size
for( int j=1 ; j <= Nsim ; j++ ){ //loop over all indices
    if( (j-1)%(t+1) == t/2 ) continue; //skip this 'old' sampling probability
    p[idx] = (double) (j-0.5) / Nsim; //new sampling probability
    idx++; //increase index by one
}
    
```

Fig. 5. Fragment of C code responsible for computation of the additional sampling probabilities p_{add} .

skipped: $j = 2, 5, 8, 11, \dots$ while the remaining indices $j = 1; 3, 4; 6, 7; 9, 10; \dots$ are used to obtain p_{add} . The fragment of C code in Figure 5 shows a cycle that fills the vector of sampling probabilities p_{tot} with the additional part p_{add} .

In order to illustrate the regular distribution of the sampling probabilities, Figure 4 (left) shows the situation for an initial design with just one simulation ($N_0 = 1$) and the refinement factor $t = 2$. Figure 4 (right) illustrates the situation for $N_{old} = 2$ and $t = 4$ (four offsprings). This can be advantageous in cases when, after performing N_{old} analyses, the analyst plans to extend the sample size more rapidly than just by doubling the previous number. Or, for example, quadrupling N_{old} may be more desirable than doubling it and immediately after that doubling N_{sim} again.

4 SAMPLE SIZE EXTENSION ALGORITHM: MULTIVARIATE SAMPLING AND CONTROL OVER DEPENDENCE

The proposed concept of the HLHS method for a single variable can be easily extended to a multivariate setting. Suppose the problem to be analyzed via sampling features N_{var} variables. The initial LHS design, with N_{old} sampling probabilities p_{old} , has already been performed (sample ordering has already been optimized to conform to the target dependence structure). Suppose also that this design has already been utilized

and the N_{old} results with function $g(X)$ are obtained. The points in the existing design must therefore remain unchanged.

Now, the new sampling probabilities p_{add} are available via the application of the refinement of the grid of sampling probabilities (see the preceding section). These new sampling probabilities will be used in Equation (7) to obtain the additional sample. The only problem is thus to achieve the optimal reordering of the additional sample set for each random variable (row) in such a way that the aggregated sample matches the target multivariate structure as much as possible. It is proposed that the optimal pairing (dislocation of the points in N_{var} -dimensional space) be achieved by application of the above-mentioned combinatorial optimization algorithm described in Vořechovský and Novák (2009).

In fact, the algorithm performs the same kind of job as in the preceding design with N_{old} points. The only difference is that mutual ordering can only be changed for the new sampling points, that is, the points with the indices $N_{old} < j, k \leq N_{sim}$; see Figure 1. This can be achieved very easily in the above-mentioned algorithm by specifying the lower bounds on the indices j, k for swapped values.

Of course, when optimizing the mutual ordering of the additional sample set, the objective function (e.g., the correlation error) also takes into account the preceding, old sample set. In this way, any possible errors in correlation that may have appeared in the old (smaller) design are automatically reduced because the algorithm

for correlation control compensates for them while optimizing the ordering of the new sampling probabilities.

A valuable aspect of this approach is that the marginal distributions of the original random vectors remain intact, and the algorithm merely provides a key to re-ordering the elements of the original random vectors. In this sense, the proposed algorithm is a truly “distribution-free” algorithm, as it does not depend on the distribution functions featured in the problem.

Let us focus on the common situation case in which the correlation error is the objective function to be minimized and the correlation estimator is either Pearson linear or Spearman’s rank correlation coefficient. In both cases, correlation between a pair of variables, X and Y , represented by vectors of N_{sim} values x_j and y_j , can be calculated as the *dot product* of two vectors. This can be shown using the linear Pearson’s correlation; computation of the Spearman correlation takes place in an identical manner, except that the sample set is replaced by integer ranks; see, for example, Vořechovský (2012a). The linear Pearson’s correlation estimator for the data representing a pair of random variables is given by:

$$\rho_{xy} = \frac{\sum_{j=1}^{N_{\text{sim}}} (x_j - \bar{x})(y_j - \bar{y})}{\sqrt{\sum_{j=1}^{N_{\text{sim}}} (x_j - \bar{x})^2} \sqrt{\sum_{j=1}^{N_{\text{sim}}} (y_j - \bar{y})^2}} \quad (14)$$

For the correlation control algorithm, the values can be temporarily standardized by subtracting the mean value and dividing this by the standard deviation. After that, the correlation coefficient reads:

$$\rho_{xy} = \frac{\sum_{j=1}^{N_{\text{sim}}} x_j y_j}{(N_{\text{sim}} - 1)} \quad (15)$$

If all the values in the sample sets are further divided by $\sqrt{N_{\text{sim}} - 1}$, the correlation can be computed simply as the dot product:

$$\rho_{xy} = \sum_{j=1}^{N_{\text{sim}}} x_j y_j = \underbrace{\sum_{j=1}^{N_{\text{old}}} x_j y_j}_{\text{fixed ordering}} + \underbrace{\sum_{j=N_{\text{old}}+1}^{N_{\text{sim}}} x_j y_j}_{\text{ordering to be optimized}} \quad (16)$$

Any swap of a pair of values with indices j, k of any variable i only influences the $N_{\text{var}} - 1$ correlations in the estimated correlation matrix A because the affected variable i has correlations with $N_{\text{var}} - 1$ variables; see Figure 1 (right). To update each of these $N_{\text{var}} - 1$ correlation coefficients, one multiplication and three subtractions must be computed:

$$\begin{aligned} \rho_{xy}^{\text{upd}} &= \rho_{xy} - x_j y_j - x_k y_k + x_j y_k + x_k y_j \\ &= \rho_{xy} - (x_j - x_k)(y_k - y_j) \end{aligned} \quad (17)$$

Therefore, the actual number of simulations does not influence the speed of the algorithm and the fact that part of the sample is fixed is not a problem.

Once the ordering of the additional part of the sample is optimized, the resulting sampling plan uses the same sampling probabilities as a sample that would be simulated at N_{sim} by classical LHS, that is, in one step. The only source of different performance may lie in the fact that the optimization of mutual ordering has been performed for the two subsamples successively. It can be expected that, the performance of the aggregated sample set determined during the estimation of the statistical characteristics of the studied function $g()$, can only be equally as good as in standard LHS at the same sample size. It can be expected that HLHS only provides just slightly worse results than LHS when the sample size N_{old} is extremely small. This is because the correlation errors (and also other measures, such as spatial uniformity) decrease with increasing sample size.

The following paragraph is focused on the case in which the shuffling algorithm controls *correlations*. As shown by Vořechovský and Novák (2009) and also in Vořechovský (2012c), the subsequent addition of samples has no negative impact on the quality of the correlation structure of the resulting sample set. This is also true for random ordering (see Vořechovský, 2012a). It should be noted that when $N_{\text{sim}} \leq N_{\text{var}}$, which can easily happen especially in initial designs, the estimated correlation matrix, A , is singular and positive semidefinite. The associated correlation error drastically decreases when N_{sim} exceeds N_{var} . In these situations, the average error in correlation is approximately $N_{\text{sim}}^{-5/2} N_{\text{var}}$ with the coefficient of variation $1/N_{\text{var}}$ (Vořechovský, 2011). More information on this issue can be found in Vořechovský (2012c).

This potential error, a problem stemming from the lower flexibility available due to successive sampling, is visualized in Figure 6. The figure shows the evolution of a bivariate sample selection in HLHS with uniformly distributed variables (or sampling probabilities). The left-hand side shows the selection with uncorrelated variables ($T = 0$), while the middle column has $T = -0.9$. Both cases start with the initial design featuring only one sampling point, and the extensions double the old sample size. During the first extension, there are only two ways to pair the two new coordinates, leading either to perfect positive or negative dependence. During extension no. 2, this dependency is efficiently suppressed by balancing the correlation. However, if the correlation control algorithm would have the freedom

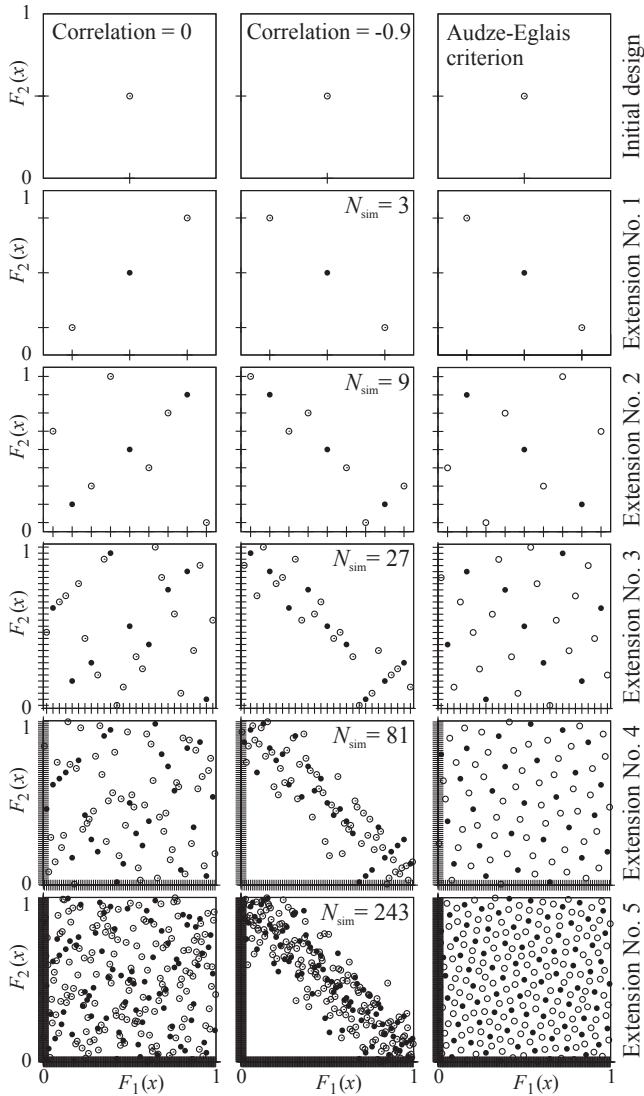


Fig. 6. Evolution of bivariate sampling probabilities (or samples of uniform variables) with $N_0 = 1, t = 2$. Solid circles represent the old sample set and empty circles represent the additional points. Left column: Statistically independent case. Middle column: Negatively correlated variables. Right column: Audze-Eglais criterion (potential energy).

to pair all the sampling probabilities, the result would be slightly better. This problem disappears very quickly as the sample size increases. Yet, for small sample sizes, the flexibility provided by HLHS may be offset by a small decrease in the ability to fulfill the correlation criteria.

It can be argued that a good design for a computer experiment should provide information about all sectors of the experimental region. Uneven designs can yield predictors that are very inaccurate in sparsely observed parts of the experimental region. It can be seen

that there are several unexplored regions and also clusters of points in Figure 6 (left). The reason why this happens is that the objective function to be minimized in the pairing phase of the proposed technique is the correlation error alone, without other criteria. In order to deliver more uniform coverage of the probability space, another criterion can be used, for example, in linear combination with the correlation criterion. There are several standard criteria (Husslage, 2006; Husslage et al., 2011) that can be employed which are known from low-discrepancy sequences, minimax and maximin designs, Audze-Eglais design, or space-filling designs. The extension of the proposed algorithm to these criteria is straightforward. Figure 6 shows the evolution of a bivariate sample selection in HLHS with uniformly distributed variables, where the objective function for optimization (minimization) is the Audze-Eglais criterion (potential energy U) (Bates et al., 2003):

$$U = \sum_{j=1}^{N_{\text{sim}}} \sum_{k=j+1}^{N_{\text{sim}}} \frac{1}{L_{j,k}^2}, \quad L_{j,k}^2 = \sum_{i=1}^{N_{\text{var}}} (x_{i,j} - x_{i,k})^2 \quad (18)$$

where $L_{j,k}$ is the distance between points j and k ($j \neq k$) in N_{var} -dimensional space.

5 NUMERICAL EXAMPLES: FUNCTIONS OF RANDOM VECTORS

The following text documents the convergence of estimates of various functions with increasing sample size. In particular, the proposed HLHS method is compared to standard LHS and also to crude MCS. In all three of the compared techniques, the same algorithm for correlation control is employed. The goal is to show the extent to which the flexibility in the selection of the initial sample size in HLHS influences the performance at the final sample size N_{sim} compared to classical LHS if calculated also for N_{sim} .

It is impossible to explore all existing functions. Several test functions have been selected to represent the possible functions that may appear in practice. For all these functions, the ability to estimate the *mean value* μ_Z and *standard deviation* σ_Z of the transformed variable $Z = g(X)$ is presented.

In MCS the selection of sampling probabilities is random (it depends on sequences generated by a pseudorandom number generator). In LHS and HLHS the sampling probabilities are deterministic. However, in all three sampling techniques the pairing algorithm based on simulated annealing depends on a pseudorandom number generator. That is why all the results (μ_Z and σ_Z) are calculated repeatedly with different random number generator settings (seeds) and the averages and

sample standard deviations (sstd) are presented. This gives the reader an idea regarding the variability of the obtained estimates. Of course, MCS always delivers greater variance of estimated μ_Z and σ_Z than LHS and HLHS, which are variance reduction techniques. The number of runs with identical N_{sim} , from which the average and sstd are calculated and plotted as error bars, is 100.

The studies with HLHS are performed with various numbers of simulations in the initial design (N_0) and the design is usually hierarchically refined many times until N_{sim} reaches approximately 6,000. The refinement factor t is always set to the minimum possible value, 2.

5.1 The sum of Gaussian random variables

The distribution of the sum

$$g_{\text{sum}}(X_1, X_2) = X_1 + X_2 \quad (19)$$

of two jointly normally distributed variables, X_1 and X_2 , with Pearson's correlation ρ , is normal with a mean value of $\mu_{\text{sum}} = \mu_{X_1} + \mu_{X_2}$ and a variance of $\sigma_{\text{sum}}^2 = \sigma_{X_1}^2 + \sigma_{X_2}^2 + 2\sigma_{X_1}\sigma_{X_2}\rho$. Two cases are considered regarding Pearson's correlation, an independent case (ind) and a correlated case (cor) with $\rho = -0.9$. With no loss of generality, standardized variables are considered so that

$$\mu_{\text{sum}}^{\text{ind}} = \mu_{\text{sum}}^{\text{cor}} = 0 \quad (20)$$

$$\sigma_{\text{sum}}^{\text{ind}} = \sqrt{2} \approx 1.414214 \quad (21)$$

$$\sigma_{\text{sum}}^{\text{cor}} = 1/\sqrt{5} \approx 0.447214 \quad (22)$$

5.2 The product of independent Gaussian random variables

The PDF of the product

$$g_{\text{prod}}(X_1, X_2) = X_1 X_2 \quad (23)$$

of two independent standard normally distributed variables, X_1 and X_2 , is

$$f_{\text{prod}}(z) = \frac{1}{\pi} K_0(|z|) \quad (24)$$

where $K_n(x)$ is the modified Bessel function of the second kind. Integrating the above PDF over $(-\infty, \infty)$ for statistical moments provides the analytical zero mean and unit variance. Note that in a nonstandardized and correlated case, the mean value $\mu_{\text{prod}} = \mu_{X_1}\mu_{X_2} + \rho\sigma_{X_1}\sigma_{X_2}$ and the variance $\sigma_{\text{prod}}^2 = \mu_{X_1}^2\sigma_{X_2}^2 + \mu_{X_2}^2\sigma_{X_1}^2 + \sigma_{X_1}^2\sigma_{X_2}^2(1 + \rho^2) + 2\rho\mu_{X_1}\mu_{X_2}\sigma_{X_1}\sigma_{X_2}$.

5.3 The minima of independent Weibull random variables

The distribution of the minima (extremes):

$$g_{\text{min}}(X_1, X_2) = \min(X_1, X_2) \quad (25)$$

of $n = 2$ independent and identically distributed Weibull variables, X_1 and X_2 , with Weibull modulus m and scale parameter s , is Weibullian, with the shape parameter m (the coefficient of variation of the result remains unchanged from that of X) and the scale parameter $s_n = s \cdot n^{-1/m}$. The mean value of X involves the Gamma function Γ : $\mu_X = s \Gamma(1 + 1/m)$. The coefficient of variation reads

$$\text{cov}_X = \sqrt{\Gamma(1 + 2/m) / \Gamma^2(1 + 1/m) - 1} \quad (26)$$

The mean value and standard deviation of the transformed variable are

$$\mu_{\text{min}} = s_n \Gamma\left(1 + \frac{1}{m}\right) = s \cdot n^{-1/m} \cdot \Gamma\left(1 + \frac{1}{m}\right) \quad (27)$$

$$\sigma_{\text{min}} = \sqrt{s_n^2 \cdot \Gamma(1 + 2/m) - \mu_{\text{min}}^2} \quad (28)$$

For the selection of scale parameter $s = 1$ and shape parameter $m = 12$ the results are

$$\mu_{\text{min}} \approx 0.904501, \quad \sigma_{\text{min}} \approx 0.091550 \quad (29)$$

This may be applied, for example, to the strength of a series system (the weakest link model).

5.4 The sum of the cosines of a pair of independent Gaussian random variables

Consider the sum of the cosines of two independent standard Gaussian variables, X_1 and X_2

$$g_{\text{cos}}(X_1, X_2) = \sum_{i=1}^{N_{\text{var}}} \cos(X_i) \quad (30)$$

The mean value and variance of this transformation equal $\mu_{\text{cos}} = N_{\text{var}} \exp(-1/2)$, $\sigma_{\text{cos}}^2 = -N_{\text{var}} \exp(-1) + N_{\text{var}} [1 + \exp(-2)]/2$. In the case of $N_{\text{var}} = 2$, the approximate values are: $\mu_{\text{cos}} \approx 1.213061$, $\sigma_{\text{cos}} \approx 0.632120$.

5.5 The sum of the squares of independent Gaussian random variables

The distribution of the sum of the squares

$$g_{\text{sqr}}(\mathbf{X}) = \sum_{i=1}^{N_{\text{var}}} X_i^2 \quad (31)$$

of independent standard Gaussian variables X_i , $i = 1, \dots, N_{\text{var}}$ is an χ -squared distribution with the mean value and standard deviation

$$\mu_{\text{sqr}} = N_{\text{var}}, \quad \sigma_{\text{sqr}} = \sqrt{2N_{\text{var}}} \quad (32)$$

5.6 The sum of the exponentials of independent Gaussian random variables

Consider the sum of the exponentials of independent standard Gaussian variables X_i , $i = 1, \dots, N_{\text{var}}$:

$$g_{\text{exp}}(\mathbf{X}) = \sum_{i=1}^{N_{\text{var}}} \exp(-X_i^2) \quad (33)$$

The mean value and standard deviation of the transformed variable are

$$\mu_{\text{exp}} = N_{\text{var}}\sqrt{3}/3 \approx 0.57735N_{\text{var}} \quad (34)$$

$$\sigma_{\text{exp}} = \sqrt{N_{\text{var}}}\sqrt{\sqrt{5}/5 - 1/3} \approx 0.33746\sqrt{N_{\text{var}}} \quad (35)$$

6 RESULTS AND DISCUSSION

In this section, the results obtained with the six test functions are discussed. The convergence has been studied with (1) just a pair of random variables (Figure 7) and (2) two functions have been selected to show the dependence of the convergence on the number of variables N_{var} ; see Figure 8. In all the plots, the analytical solutions to which the results converge are denoted by a hatched line. In most of the plots, the results for HLHS are obtained for the initial sample size $N_0 = 3$ (the lines with empty circles begin at $N_{\text{sim}} = 3$).

In both multiplots, the left-hand side presents the convergence of the estimated mean value and the right-hand plots present estimates of standard deviations.

In all the cases, the performances of LHS and HLHS in estimating the *mean value* are practically identical. The estimated mean value has almost no scatter (the variance of the estimate is reduced to practically zero). The plots also show that MCS estimates have relatively large variance that reduces with increasing sample size. The average estimates of LHS and HLHS are usually slightly biased at very small sample sizes ($N_{\text{sim}} \lesssim 10$).

In Figure 7 (left), the penultimate function g_{sqr} has been evaluated with various initial sample sizes, N_0 . The plots of *mean value* estimates overlap, and therefore it can be concluded that the number N_0 has no impact on the estimated mean value.

Figure 8 (left) also shows that the variance of MCS in estimating the *mean value* depends on the number of

random variables (even though the convergence rate is independent of N_{var}).

The situation is slightly different in the case of estimated *standard deviation*. It can be seen that the convergence of HLHS is slightly worse than that of LHS at the same (small) sample size. There are two reasons for this. First, when the sample size is very small, the correlation coefficient of the initial design in HLHS can be far from that which is desired. Even if the HLHS method compensates for the errors upon adding new sample points, a correlation coefficient obtained from standard LHS with a larger sample produced all at once may be better. This potential error in correlation (the uniformity of coverage of the sampling region with respect to the joint PDF) may distort the estimates.

The second reason lies in the different method of selecting sampling probabilities used in LHS and HLHS, namely the difference between selecting the mean values of intervals (Equation 5) and selecting the medians (Equation 6). As explained and documented by Vořechovský and Novák (2009), selection of the mean values yields samples with smaller error in sstd (and the arithmetical averages [aave] match the mean values exactly). This method is therefore preferable when using LHS. In the proposed HLHS method, however, sampling is performed using the *medians*, as then the sampling probabilities form a regular grid that can be easily refined.

In Figures 7 (right) and 8 (right), it can be seen that the average of the estimated *standard deviation* is usually biased for all three methods when N_{sim} is small. Moreover, Figure 8 (right) shows that the bias in the *standard deviation* estimated by LHS and HLHS depends on N_{var} . The more random variables there are, the greater the bias.

Figure 7 (top row) compares the convergence for the estimates of a sum of two random variables that are either independent or highly (negatively) correlated. It can be seen that the quality of estimates obtained with LHS and HLHS does not depend on the correlation between the input variables. However, the average estimate of MCS is somewhat biased for small N_{sim} in the correlated case.

While efficient sampling strategies, such as optimized LHS, may allow a target accuracy to be reached with a minimal number of simulation runs, the ability to halt the simulations when sufficient accuracy has been attained also reduces the computational cost. So, given the choice of a sampling method for studying a computer model, a natural yet difficult question is how many simulation runs to use. This issue is addressed in Schuyler's (1997) article on "how many trials is enough" and also in Gilman's (1968) brief survey on stopping rules. A detailed discussion on measuring the sampling

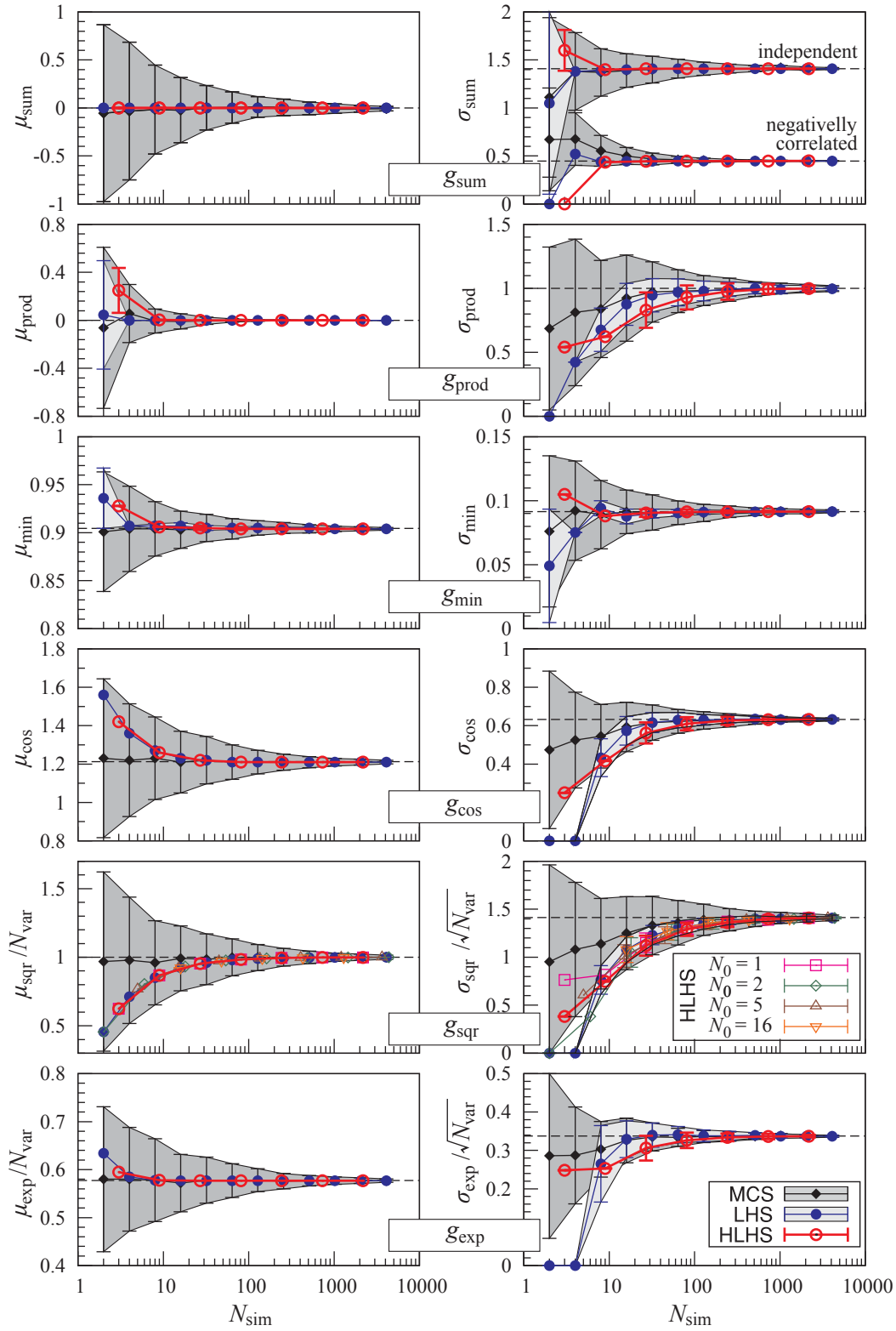


Fig. 7. Convergence of estimates to the analytical mean and standard deviation for six functions g of a pair of random variables. Left: The mean value of g . Right: The standard deviation of g .

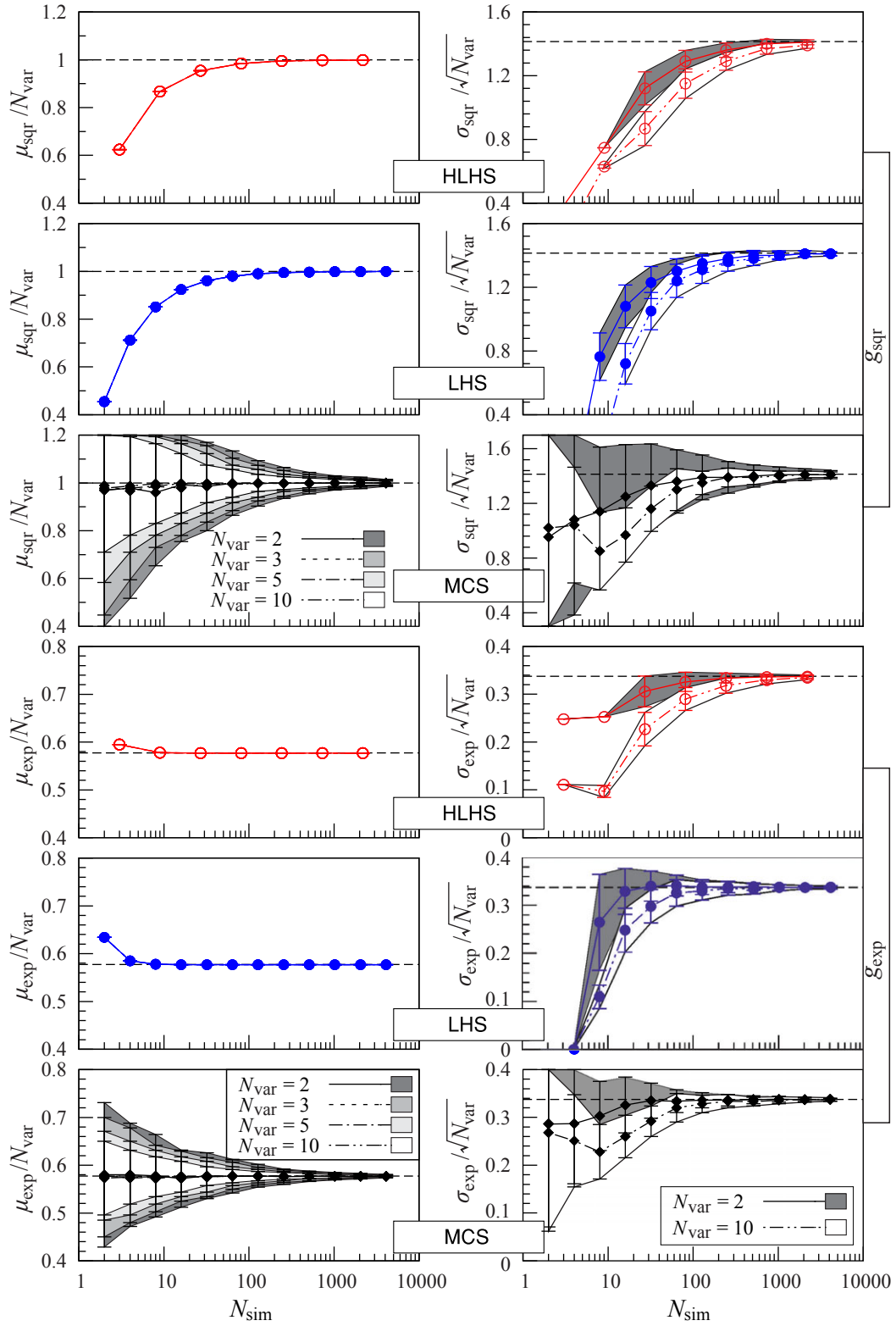


Fig. 8. Convergence of estimates to the analytical mean and standard deviation for two selected functions of various numbers of uncorrelated variables. Left: The mean value of g . Right: The standard deviation of g .

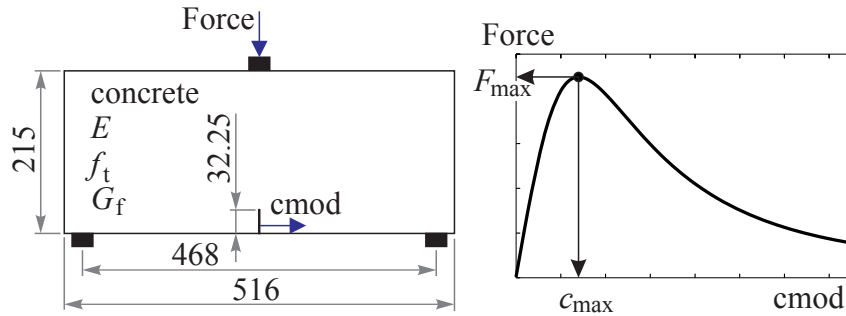


Fig. 9. Three point bending of notched concrete specimens. Left: Geometry. Right: Typical calculated diagram and the definition of output variables.

convergence in MCS, LHS, and replicated LHS with the aim of assessing the accuracy with which decisions can be made on when to halt the simulation process can be found in a recent paper by Janssen (2013).

To conclude, the performance of the proposed HLHS method is almost identical to that of standard LHS when carried out with the same number of model evaluations. The small decrease in the accuracy of HLHS is, for practical problems involving time-consuming model evaluations, balanced by the great advantage of HLHS, which is its ability to increase the sample size adaptively based on current progress.

The fact that the sample size increases relatively quickly upon the addition of a new sample is the price paid for the perfect uniformity of marginal variable sampling probabilities. If the sample size increase presents a significant problem, the algorithm can be easily adjusted to deliver only replications of the sampling probabilities combined with the shuffling of mutual ranks so as to avoid repetitions of the same points in the sample space of all random variables. This can be solved for uncorrelated cases, and statistical correlation can later be induced by using the Nataf (1962) model (exploiting Cholesky transformation or orthogonal transformation using eigenvalues of the target correlation matrix T).

7 NUMERICAL EXAMPLE: FRACTURE-MECHANICS ANALYSES

The following numerical example is included to illustrate the application of the suggested technique to a realistic problem involving complex analysis. The problem of the initiation and growth of cracks in notched concrete specimens loaded in three point bending has been selected. Three material properties are considered as random variables—tensile strength f_t , Young's modulus E , and fracture energy G_f . The analysis aims at es-

timating the mean value, standard deviation, and also the PDF of two response variables, namely the peak force, F_{max} , and the crack mouth opening displacement (CMOD) corresponding to the peak force, c_{max} . The shape of the concrete specimens and the inputs and response variables are depicted in Figure 9. The selected concrete specimen shape has been tested experimentally (Hoover et al., 2013) as a part of a larger experimental setup focused on the size effect phenomenon.

The simulated response of specimens is calculated by employing nonlinear finite element analysis as implemented in the OOFEM software package (Patzák, 2000; Patzák and Bittnar, 2001; Patzák and Rypel, 2012). OOFEM is an Object Oriented Finite Element Solver with an impressive range of options and good documentation. The progressive failure that is crack growth is modeled by employing the isotropic damage model for tensile failure (Idm1) implemented in the OOFEM program. This isotropic damage model assumes that stiffness degradation is isotropic, that is, stiffness moduli corresponding to different directions decrease proportionally and independently of the loading direction. Equivalent strain, which serves as a scalar measure of the strain tensor, is defined according to the Mazars model; the definition is based on the norm of the positive part of the strain. Since the growth of damage leads to softening and induces localization of the dissipative process, attention must be paid to proper regularization. The model is local, and the damage law with exponential softening is adjusted according to the element size (crack-band approach).

The analyses are relatively time consuming, partly due to the fine mesh used. The band of ligament elements above the notch of width 1.5 mm are squares of approximately the same size, and therefore there is a row of 123 finite elements. In the rest of the domain, squared elements of size 4.3 mm are used so that the depth of the specimen is discretized into 50 finite elements. The same element size is used for the steel blocks

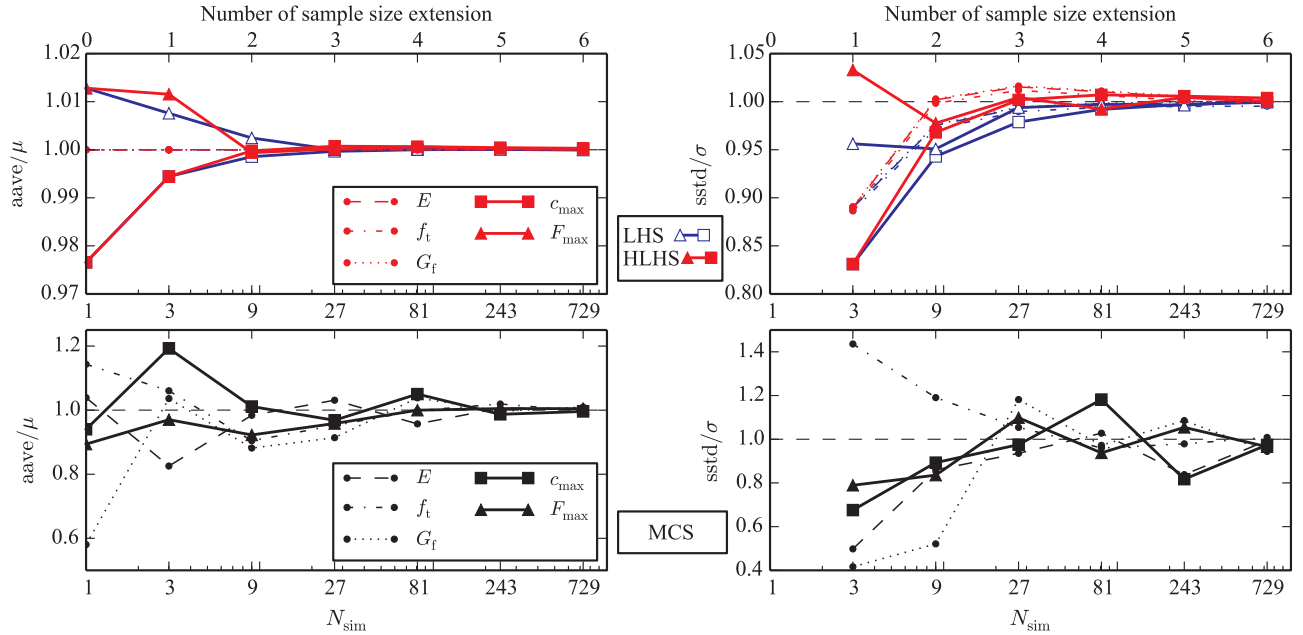


Fig. 10. Convergence of estimated moments (standardized by the values from Table 1) of input and output variables. Left: Arithmetical averages (aave). Right: Sample standard deviations (sstd).

supporting the specimen and also for the block at the top of it (block dimensions: 27.5×17.2 mm). Each analysis takes approximately one hour on a modern PC.

As with the numerical examples presented in Section 5, three types of Monte Carlo analysis were performed, namely crude Monte Carlo Sampling (MCS), standard LHS, and the proposed HLHS method. The analyses with MCS and LHS were performed with all the sample sizes N_{sim} that appear in progressively extended sample sizes in HLHS: $N_{\text{sim}} = 3^{(i)} = 1, 3, 9, 27, 81, 243, 729$ ($i = 0, \dots, 6$). Therefore, the least number of simulations in total were performed with HLHS, where the total sample size equalled 729. The total number of evaluations of the model performed with LHS and MCS was the sum of all the sample sizes, $\sum 3^i = 1,093$. Since the simulations are time consuming, only one run of all the sets of simulations has been performed for each technique, and so information on the statistical scatter of estimated parameters is not available. The presented numerical examples mimic the situation for which HLHS is designed: the user progressively adds time-expensive simulations with the intention of keeping the total number of model evaluations low. The evolution of the target estimated statistical parameters, possibly accompanied with the testing of hypotheses at the target significance level, gives a hint as to the sample size which will be revealed as sufficient.

Table 1 summarizes the input variables that are considered to be random variables, together with the pa-

Table 1
Description of input and output variables

Type	Variable name and unit	Mean value	Std. dev.	c.o.v.	PDF
Input	E (GPa)	36.5	5.48	0.15	Normal
	f_t (MPa)	4.38	0.88	0.2	Normal
	G_f (N/m)	60	18	0.3	Normal
Output	c_{max} (μm)	107*	17.3*	0.16*	Gumbel*
	F_{max} (kN)	4.43*	0.83*	0.19*	Normal*

Stars designate results based on numerical estimations. c.o.v. = coefficient of variation.

rameters of the random variables. The table also displays estimates of the statistical moments of the two output variables. The distribution functions of the output variables are best fits selected from a list of distribution functions available in FReET software (Novák et al., 2003; Novák et al., 2014) using the goodness-of-fit (Kolmogorov-Smirnov) test. The three input variables were considered correlated; the correlations appear in Figure 11.

Figure 10 presents the convergence of estimated statistical parameters of the input [output] variables to the target [accurate] values. In particular, the figure presents the convergence of the aave and sstd, both standardized by the exact values. It can be seen that in the case of MCS (bottom row), the estimations vary for various sample sizes (compared with the variance

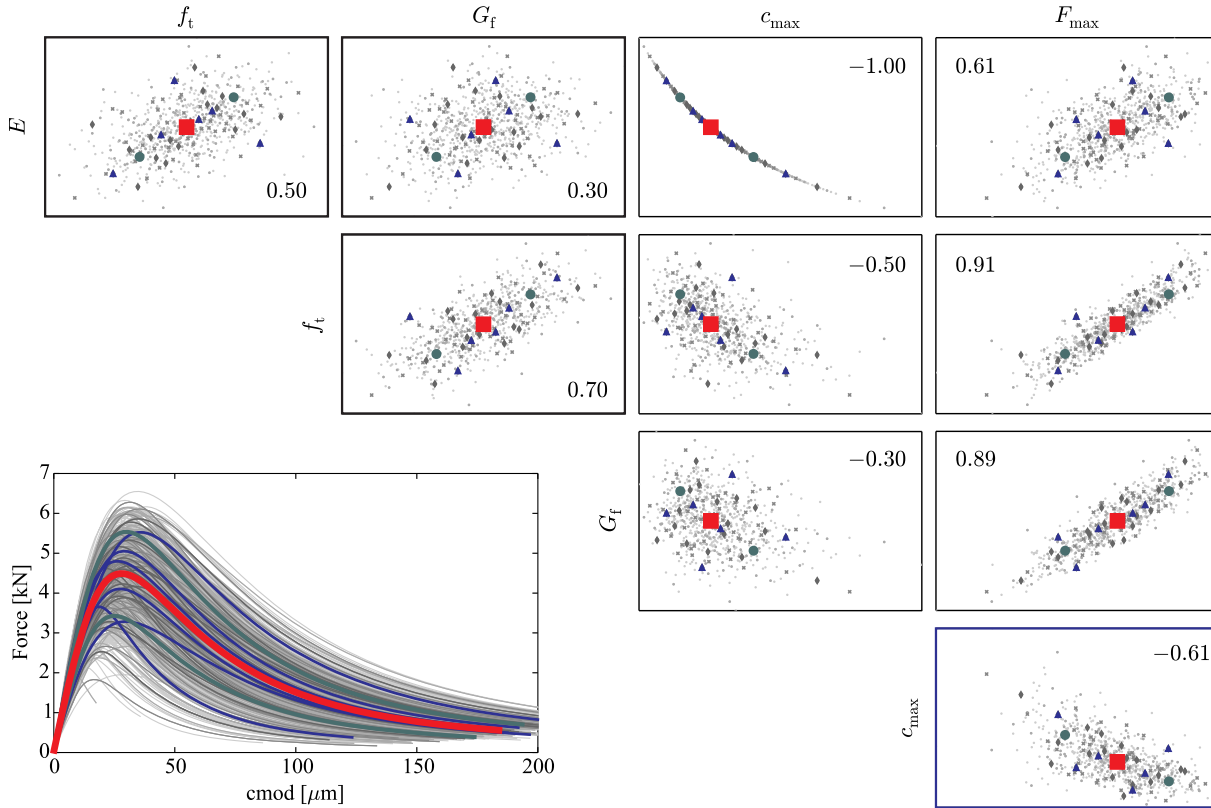


Fig. 11. Top right matrix: Evolution of bivariate scatterplots obtained via HLHS accompanied with the values of Spearman rank order correlation. Symbol sizes correspond to the numbers of sampling size extensions. Bottom left: Evolution of a bundle of calculated force (CMOD) diagrams obtained via HLHS. The thick lines correspond to initial simulations

expressed using the error bars in previous examples); the error can easily reach 10%. LHS and HLHS both yield much better results than MCS. The accuracy for LHS and HLHS is about the same. Reasonable results for the standard deviation can already be obtained for $N_{\text{sim}} = 81$ (the fourth extension of the sample size). The sample averages of the inputs are identical and exact in these two techniques (symmetrical sampling) but the sstd evolve in a slightly different way. The reason is that while HLHS starts by sampling the *mean value* (Equation 5), the *medians* of intervals are used (Equation 6) for the sample size extension in order to guarantee the even distribution of new sampling probabilities. The results obtained with LHS are gained with sampling the mean values of intervals (see also the discussion in Section 6). Otherwise, the techniques yield almost identical results. Note, however, that in LHS exhausting all previous sample sizes until the fourth extension in pilot sets would require $N_{\text{sim}} = 1 + 3 + 9 + 27 + 81 = 121$ model evaluations, while in HLHS only 81 evaluations would need to be performed.

The evolving bundle of diagrams calculated with HLHS is also interesting; see bottom left in Figure 11.

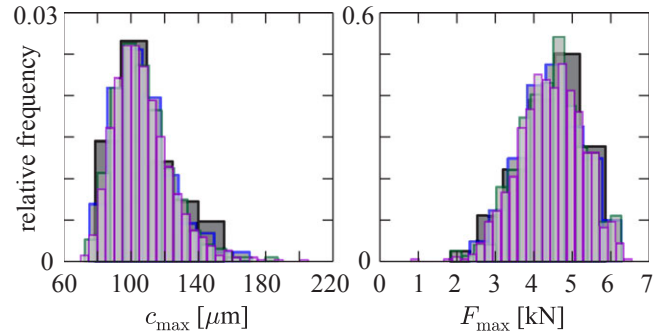


Fig. 12. Evolution of empirical histograms of output variables obtained via HLHS.

The initial simulation with the mean values is depicted by a thick line, while the second level adds two thinner curves, etc. The scatterplots in Figure 11 show the evolving selection of sampling points for all pairs of input and also output variables. This information provides control over input correlations and also serves as an important source of information on (1) the dependence patterns between inputs and outputs and also (2)

between the two output variables. For example, it confirms the intuitively acceptable fact that the CMOD at peak load, c_{\max} , exhibits perfect negative dependence on the E modulus. On the other hand, the peak force F_{\max} is strongly correlated with both tensile strength f_t and fracture energy G_f . This information can also be visualized while extending the sample size, and the significance of the calculated sensitivities (in the form of correlations) can easily be calculated.

The estimated PDF of the outputs may be important information which can be gained using empirical histograms. The evolution of these histograms is visualized in Figure 12. Better information on the tails can be obtained by adding more sampling points. This can be done easily just by extending the sample size in HLHS.

8 CONCLUSIONS

The article proposes a technique for the sample size extension of an LH-sample in which the new sample points are selected based on the locations of the available sample points (without exploiting information from the obtained results). It is shown that the proposed adaptive technique HLHS yields a result approximately equally as good as that obtained from standard LHS for the same number of model evaluations. The computational advantage lies in the possibility to begin with a small sample and extend it if necessary. The method is designed for small sample sets (from tens to a maximum of thousands of simulations) that can be extended and merged together to constitute a consistent sample set and preserve the capability to provide the variance reduction of estimates at the same time.

It is proposed that the desired correlation or other types of multivariate structure description (copulas, discrepancy, space-filling criteria) be induced by the previously developed combinatorial optimization technique.

Adaptive refinement can be performed as long as some stopping criteria are met. The criteria for termination can be especially (1) the user's decision based, for example, on material or computing resources; and (2) the statistical significance of an arbitrary parameter.

The typical application of the proposed HLHS is in situations involving a computer-based model in which it is impossible to find a way (either closed form or numerical) of performing the necessary transformation of variables, and where the model is expensive to run in terms of computing resources and time. Examples of applications include simulations of random fields, the design of physical or computer experiments, pilot numerical studies of complicated functions of random variables, the progressive learning of neural networks, etc.

The method is implemented in FReET software (Novák et al., 2003; Novák et al., 2014).

ACKNOWLEDGMENTS

The author acknowledges financial support provided by the Czech Ministry of Education, Youth and Sports under project No. LH12062 and also support provided by the Czech Science Foundation under project no. GA14-10930S (SPADD). The author thanks his colleague Václav Sadílek and former student František Černík for their help with numerical simulations presented in the article.

REFERENCES

- Adeli, H. & Park, H. S. (1996), Hybrid CPN–neural dynamics model for discrete optimization of steel structures, *Computer-Aided Civil and Infrastructure Engineering*, **11**(5), 355–66.
- Andres, T. (1997), Sampling methods and sensitivity analysis for large parameter sets, *Journal of Statistical Computation and Simulation*, **57**(1-4), 77–110.
- Anoop, M. B., Raghuprasad, B. K. & Balaji Rao, K. (2012), A refined methodology for durability-based service life estimation of reinforced concrete structural elements considering fuzzy and random uncertainties, *Computer-Aided Civil and Infrastructure Engineering*, **27**(3), 170–86.
- Bates, S., Siens, J. & Langley, D. (2003), Formulation of the Audze-Eglaiss Uniform Latin Hypercube design of experiments, *Advances in Engineering Software*, **34**(8), 493–506.
- Bažant, Z. P., Pang, S. D., Vořechovský, M. & Novák, D. (2007), Energetic-statistical size effect simulated by SFEM with stratified sampling and crack band model, *International Journal for Numerical Methods in Engineering*, **71**(11), 1297–320.
- Blatman, G. & Sudret, B. (2010), An adaptive algorithm to build up sparse polynomial chaos expansions for stochastic finite element analysis, *Probabilistic Engineering Mechanics*, **25**(2), 183–97.
- Brząkała, W. & Puła, W. (1996), A probabilistic analysis of foundation settlements, *Computers and Geotechnics*, **18**(4), 291–309.
- Cacuci, D. G. (2003), *Sensitivity & Uncertainty Analysis, Volume 1: Theory*, 1st edn, Chapman and Hall/CRC, Boca Raton, FL.
- Chudoba, R., Sadílek, V., Rypal, R. & Vořechovský, M. (2013), Using python for scientific computing: an efficient and flexible evaluation of the statistical characteristics of functions with multivariate random inputs, *Computer Physics Communications*, **184**(2), 414–27.
- Conover, W. (1975), On a better method for selecting input variables. Unpublished Los Alamos National Laboratories manuscript, reproduced as Appendix A of “Latin Hypercube Sampling and the Propagation of Uncertainty in Analyses of Complex Systems” by J.C. Helton and F.J. Davis, Sandia National Laboratories report SAND2001-0417, Albuquerque, NM and Livermore, CA.

- Dai, H., Zhang, H., Wang, W. & Xue, G. (2012), Structural reliability assessment by local approximation of limit state functions using adaptive Markov chain simulation and support vector regression, *Computer-Aided Civil and Infrastructure Engineering*, **27**(9), 676–86.
- Duthie, J. C., Unnikrishnan, A. & Waller, S. T. (2011), Influence of demand uncertainty and correlations on traffic predictions and decisions, *Computer-Aided Civil and Infrastructure Engineering* **26**(1), 16–29.
- Frank, P. M. (1978), *Introduction to System Sensitivity Theory*, Academic Press Inc., State University of New York at Stony Brook, Stony Brook, NY.
- Fuggini, C., Chatzi, E. & Zangani, D. (2013), Combining genetic algorithms with a meso-scale approach for system identification of a smart polymeric textile, *Computer-Aided Civil and Infrastructure Engineering*, **28**(3), 227–45.
- Gilman, M. (1968), A brief survey of stopping rules in Monte Carlo simulations, in *Proceedings of the Second Conference on Applications of Simulations*, New York, NY.
- Graf, W., Freitag, S., Sickert, J.-U. & Kaliske, M. (2012), Structural analysis with fuzzy data and neural network based material description, *Computer-Aided Civil and Infrastructure Engineering*, **27**(9), 640–54.
- Hammersley, J. M. & Handscomb, D. C. (1964), *Monte Carlo Methods*, Taylor & Francis, Methuen, London.
- Hansen, C. W., Helton, J. C. & Sallaberry, C. J. (2012), Use of replicated Latin hypercube sampling to estimate sampling variance in uncertainty and sensitivity analysis results for the geologic disposal of radioactive waste, *Reliability Engineering and System Safety*, **107**, 139–48.
- Hegenderfer, J. & Atamturktur, S. (2012), Prioritization of code development efforts in partitioned analysis, *Computer-Aided Civil and Infrastructure Engineering*, **28**(4), 289–306.
- Helton, J. C. & Davis, F. J. (2002), *Latin Hypercube Sampling and the Propagation of Uncertainty in Analyses of Complex Systems*, Technical Report, SAND2001-0417, Sandia National Laboratories Albuquerque, NM and Livermore, CA.
- Hoover, C. G., Bažant, Z. P., Vorel, J., Wendner, R. & Hubler, M. H. (2013), Comprehensive concrete fracture tests: description and results, *Engineering Fracture Mechanics*, **114**, 92–103.
- Hsiao, F.-Y., Wang, S.-H., Wang, W.-C., Wen, C.-P. & Yu, W.-D. (2012), Neuro-fuzzy cost estimation model enhanced by fast messy genetic algorithms for semiconductor hookup construction, *Computer-Aided Civil and Infrastructure Engineering*, **27**(10), 764–81.
- Huntington, D. E. & Lyrantzis, C. S. (1998), Improvements to and limitations of Latin Hypercube Sampling, *Probabilistic Engineering Mechanics*, **13**(4), 245–53.
- Husslage, B. (2006), Maximin designs for computer experiments, Ph.D. thesis, Tilburg University.
- Husslage, B. G. M., Rennen, G., van Dam, E. R. & den Hertog, D. (2011), Space-filling Latin hypercube designs for computer experiments, *Optimization and Engineering*, **12**(4), 611–30.
- Iman, R. C. & Conover, W. J. (1980), Small sample sensitivity analysis techniques for computer models with an application to risk assessment, *Communications in Statistics: Theory and Methods*, **A9**(17), 1749–842.
- Janssen, H. (2013), Monte-Carlo based uncertainty analysis: sampling efficiency and sampling convergence, *Reliability Engineering and System Safety*, **109**, 123–32.
- Johnson, M. E. (1987, February), *Multivariate Statistical Simulation: A Guide to Selecting and Generating Continuous Multivariate Distributions* (Wiley Series in Probability and Mathematical Statistics), John Wiley & Sons, New York, NY.
- Kalos, M. H. & Whitlock, P. A. (1986), *Monte Carlo Methods*. John Wiley & Sons, New York, NY.
- Katafygiotis, L. S. & Papadimitriou, C. (1996), Dynamic response variability of structures with uncertain properties, *Earthquake Engineering & Structural Dynamics*, **25**(8), 775–93.
- Keramat, M. & Kielbasa, R. (1997), Efficient average quality index of estimation of integrated circuits by Modified Latin Hypercube Sampling Monte Carlo (MLHSMC), in *IEEE International Symposium on Circuits and Systems*, Hong Kong, pp. 1–4.
- Li, G., Rosenthal, C. & Rabitz, H. (2001), High dimensional model representations, *The Journal of Physical Chemistry A*, **105**(33), 7765–77.
- Marano, G. C., Quaranta, G. & Monti, G. (2011), Modified genetic algorithm for the dynamic identification of structural systems using incomplete measurements, *Computer-Aided Civil and Infrastructure Engineering*, **26**(2), 92–110.
- McKay, M. D., Conover, W. J. & Beckman, R. J. (1979), A comparison of three methods for selecting values of input variables in the analysis of output from a computer code, *Technometrics* **21**, 239–45.
- Mead, R. & Pike, D. J. (1975), A biometrics invited paper. A review of response surface methodology from a biometric viewpoint, *Biometrics*, **31**(4), 803.
- Myers, R. (1999), Response surface methodology – current status and future directions, *Journal of Quality Technology*, **31**(1), 30–44.
- Myers, R., Montgomery, D., Vining, G., Borror, C. & Kowalski, S. (2004), Response surface methodology: a retrospective and literature survey, *Journal of Quality Technology*, **36**(1), 53–77.
- Myers, R. H. (1971), *Response Surface Methodology*, Allyn and Bacon, Inc., Boston, MA.
- Nataf, A. (1962), Détermination des distributions de probabilités dont les marges sont donnés, *Comptes Rendus de L'Académie des Sciences*, **225**, 42–3.
- Novák, D. & Lehký, D. (2006), ANN inverse analysis based on stochastic small-sample training set simulation, *Engineering Applications of Artificial Intelligence*, **19**(7), 731–40.
- Novák, D., Vořechovský, M. & Rusina, R. (2003), Small-sample probabilistic assessment – FREET software, in A. Der Kiureghian, S. Madanat, and J. M. Pestana (eds.), *ICASP'09: International Conference on Applications of Statistics and Probability in Civil Engineering*, San Francisco, USA. Millpress, Rotterdam, Netherlands, pp. 91–6.
- Novák, D., Vořechovský, M. & Teplý, B. (2014), FREET: software for the statistical and reliability analysis of engineering problems and FREET-D: degradation module, *Advances in Engineering Software*, **72**, 179–92.
- Olsson, A., Sandberg, G. & Dahlblom, O. (2003), On Latin Hypercube Sampling for structural reliability analysis, *Structural Safety*, **25**(1), 47–68.
- Panakkat, A. & Adeli, H. (2009), Recurrent neural network for approximate earthquake time and location prediction using multiple seismicity indicators, *Computer-Aided Civil and Infrastructure Engineering*, **24**(4), 280–92.

- Patzák, B. (2000), OOFEM project home page. Available at: <http://www.oofem.org>, accessed January 1, 2014.
- Patzák, B. & Bittnar, Z. (2001), Design of object oriented finite element code, *Advances in Engineering Software*, **32**(10-11), 759–67.
- Patzák, B. & Rypl, D. (2012), Object-oriented, parallel finite element framework with dynamic load balancing, *Advances in Engineering Software*, **47**(1), 35–50.
- Qian, P. Z. G. (2009), Nested Latin hypercube designs, *Biometrika*, **96**(4), 957–70.
- Rabitz, H. & Ali, Á. F. (1999), General foundations of high-dimensional model representations, *Journal of Mathematical Chemistry* **25**(2–3), 197–233.
- Rabitz, H., Kramer, M. & Dacol, D. (1983), Sensitivity analysis in chemical kinetics, *Annual Review of Physical Chemistry*, **34**(1), 419–61.
- Reuter, U. & Möller, B. (2010), Artificial neural networks for forecasting of fuzzy time series, *Computer-Aided Civil and Infrastructure Engineering*, **25**(5), 363–74.
- Rubenstein, R. Y. (1981), *Simulation and the Monte Carlo Method*, John Wiley & Sons, New York, New Press, Oxford.
- Sacks, J., Welch, W. J., Mitchell, T. J. & Wynn, H. P. (1989), Design and analysis of computer experiments, *Statistical Science*, **4**(4), 409–23.
- Sadeghi, N., Fayek, A. R. & Pedrycz, W. (2010), Fuzzy Monte Carlo simulation and risk assessment in construction, *Computer-Aided Civil and Infrastructure Engineering*, **25**(4), 238–52.
- Sallaberry, C., Helton, J., & Hora, S. (2008), Extension of Latin hypercube samples with correlated variables, *Reliability Engineering and System Safety*, **93**(7), 1047–59.
- Schuyler, J. R. (1997), Monte Carlo stopping rule (Part 1 and Part 2). Available at: <http://www.maxvalue.com/tip025.htm>, accessed January 1, 2014.
- Sobol', I. M. (1994), *A Primer for the Monte Carlo Method*. CRC Press, Boca Raton, FL.
- Stein, M. (1987), Large sample properties of simulations using Latin Hypercube Sampling, *Technometrics*, **29**(2), 143–51.
- Tamás, T. (1990), Sensitivity analysis of complex kinetic systems. Tools and applications, *Journal of Mathematical Chemistry*, **5**(3), 203–48.
- Tong, C. (2006), Refinement strategies for stratified sampling methods, *Reliability Engineering and System Safety*, **91**(10–11), 1257–65.
- Vořechovský, M. (2006), Hierarchical Subset Latin Hypercube Sampling, in S. Vejvoda et al. (eds.), *PPK'06: Pravděpodobnost porušování konstrukcí*, Brno, Czech Republic, pp. 285–98. Brno University of Technology, Faculty of Civil Engineering and Faculty of Mechanical Engineering & Ústav aplikované mechaniky Brno, s.r.o. & Asociace strojních inženýru & TERIS, a.s., pobočka Brno.
- Vořechovský, M. (2008), Simulation of simply cross correlated random fields by series expansion methods, *Structural Safety*, **30**(4), 337–63.
- Vořechovský, M. (2009), Hierarchical Subset Latin Hypercube Sampling for correlated random vectors, in B. Topping and Y. Tsompanakis (eds.), *Proceedings of the First International Conference on Soft Computing Technology in Civil, Structural and Environmental Engineering*, Madeira, Portugal, Civil-Comp Proceedings: 92, Stirlingshire, Scotland, pp. 17 pages, CD-ROM. Civil-Comp Press.
- Vořechovský, M. (2011), Correlation in probabilistic simulation, in M. H. Faber, J. Köhler, and K. Nishijima (eds.), *ICASP'11: Proceedings of the Applications of Statistics and Probability in Civil Engineering*, Zürich, Switzerland, Cerra: Taylor & Francis Group, London, pp. 2931–9.
- Vořechovský, M. (2012a), Correlation control in small sample Monte Carlo type simulations II: analysis of estimation formulas, random correlation and perfect uncorrelatedness, *Probabilistic Engineering Mechanics*, **29**, 105–20.
- Vořechovský, M. (2012b), Extension of sample size in Latin hypercube sampling—methodology and software, in A. Strauss, D. Frangopol, and K. Bergmeister (eds.), *Proceedings of the 3rd Symposium on Life-Cycle and Sustainability of Civil Infrastructure Systems*, Vienna, Austria, IALCCE, Vienna, BOKU University, Vienna: CRC Press/Balkema, pp. 2403–10.
- Vořechovský, M. (2012c), Optimal singular correlation matrices estimated when sample size is less than the number of random variables, *Probabilistic Engineering Mechanics*, **30**, 104–16.
- Vořechovský, M. & Novák, D. (2009), Correlation control in small sample Monte Carlo type simulations I: a simulated annealing approach, *Probabilistic Engineering Mechanics*, **24**(3), 452–62.
- Vořechovský, M. & Sadílek, V. (2008), Computational modeling of size effects in concrete specimens under uniaxial tension, *International Journal of Fracture*, **154**(1–2), 27–49.
- Yuen, K.-V. & Mu, H.-Q. (2011), Peak ground acceleration estimation by linear and nonlinear models with reduced order Monte Carlo simulation, *Computer-Aided Civil and Infrastructure Engineering*, **26**(1), 30–47.
- Zhou, L., Yan, G. & Ou, J. (2013), Response surface method based on radial basis functions for modeling large-scale structures in model updating, *Computer-Aided Civil and Infrastructure Engineering*, **28**(3), 210–26.